Published in final edited form as:
J Cell Physiol. 2012 February ; 227(2): . doi:10.1002/jcp.22785.

Regulation of Endothelial Barrier Function by TGF-β type I Receptor ALK5: Potential Role of Contractile Mechanisms and Heat Shock Protein 90

Alexander S. Antonov[1], **Galina N. Antonova**[1], **Makiko Fujii**[5], **Peter ten Dijke**[6], **Vaishali Handa**[1], **John D. Catravas**[1,2,3], and **Alexander D. Verin**[1,4,*]

Peter ten Dijke: p.ten_dijke@lumc.nl

[1]Vascular Biology Center, Medical College of Georgia, Augusta, Ga 30912

[2]Department of Pharmacology and Toxicology, Medical College of Georgia, Augusta, Ga 30912

[3]Cancer Center, Medical College of Georgia, Augusta, Ga 30912

[4]Department of Medicine, Medical College of Georgia, Augusta, Ga 30912

[5]Division of Molecular Oncology, Aichi Cancer Center Research Institute, Nagoya 464-8681, Japan

[6]Dept. Molecular Cell Biology Building 2, Room R-02-022 Leiden University Medical Center, Postzone S-1-P Postbus 9600 2300 RC Leiden The Netherlands telephone: +31-71-526 9271 fax: +31-71- 5268270

Abstract

Multifunctional cytokine transforming growth factor-beta (TGF-β1) plays a critical role in the pathogenesis of acute lung inflammation by controlling endothelial monolayer permeability. TGF-β1 regulates endothelial cell (EC) functions via two distinct receptors, activin receptor-like kinase 1 (ALK1) and activin receptor-like kinase 5 (ALK5). The precise roles of ALK1 and ALK5 in the regulation of TGF-β1-induced lung endothelium dysfunction remain mostly unknown. We now report that adenoviral infection with constitutively active ALK5 (caALK5), but not caALK1, induces EC retraction and that this receptor predominantly controls EC permeability. We demonstrate that ubiquitinated ALK5 and phosphorylated heat shock protein 27 (phospho-Hsp27) specifically accumulate in the cytoskeleton fraction, which parallels with microtubule collapse, cortical actin disassembly and increased EC permeability. We have found that ALK1 and ALK5 interact with heat shock protein 90 (Hsp90). Moreover, the Hsp90 inhibitor radicicol (RA) prevents accumulation of ubiquitinated caALK5 and phospho-Hsp27 in the cytoskeletal fraction and restore the decreased EC permeability induced by caALK5. We hypothesize that specific translocation of ubiquitinated ALK5 receptor into the cytoskeleton compartment due to its lack of degradation is the mechanism that causes the divergence of caALK1 and caALK5 signaling.

Keywords

endothelial permeability; type 1 TGF-β_1 receptors; Hsp27; cytoskeleton; ubiquitin; radicicol

[*]Address correspondence to Alexander D. Verin, PhD. CB-3210, Medical College of Georgia, 1120 15th Street, Augusta, GA 30912. Phone: 706-721-1531; FAX: 706-721-9799; averin@mcg.edu.

Introduction

Acute lung injury (ALI) and acute respiratory distress syndrome (ARDS) are inflammatory disorders of the lung and are associated with high rates of morbidity and mortality. Both ALI and ARDS result from widespread lung inflammation and increased pulmonary vascular permeability (Dudek and Garcia, 2001; Parsons et al., 1989). Even with the recently successful, non-specific ventilation treatments for ALI and ARDS, there is still a tremendous need for continued research to clarify the underlying pathophysiological mechanisms and to develop approaches for specific treatments for these disorders.

Growing evidence indicates that inflammatory cytokines, such as TGF-β1, increase endothelial permeability *in vitro* and play a critical role in the development of lung edema during lung injury *in vivo* (Lucas et al., 2009; Martin et al., 1995; Pittet et al., 2001). Our previous studies (Antonov et al., 2008; Birukova et al., 2005a; Birukova et al., 2004) as well as data from other laboratories (Goldberg et al., 2002; Lu et al., 2006) demonstrated that TGF-β1-induced endothelial hyperpermeability is directly associated with activation of endothelial contractile signaling pathways. These studies elucidated the sequence of events leading from TGF-β1 signaling to the compromise of endothelial barrier function and established the principal cellular signaling pathways involved (Dudek and Garcia, 2001; Goldberg et al., 2002; Pittet et al., 2001).

TGF-β1 regulates endothelial function via two distinct receptors expressed on endothelial cells: activin receptor-like kinase 1 (ALK1) and activin receptor-like kinase 5 (ALK5) (Bertolino et al., 2005; Goumans et al., 2002; Lebrin et al., 2005; Ota et al., 2002). Although crosstalk between ALK1 and ALK5 signaling has been suggested (Finnson et al., 2008; Goumans et al., 2003a; Goumans et al., 2003b; Goumans et al., 2002), the precise role for these receptors in the regulation of TGF-β1-induced lung endothelium permeability remains mostly unknown. Recent data suggested that the receptors have different roles in regulating endothelial functions (Finnson et al., 2008; Goumans et al., 2003b; Goumans et al., 2002). Several studies imply that ALK1 receptor is important for controlling endothelial cell (EC) migration, proliferation and exstracellular matrix synthesis (Finnson et al., 2008; Goumans et al., 2003a). We have previously demonstrated that activation of ALK5 receptor is associated with an increase in EC monolayer permeability (Birukova et al., 2005a).

In this study, we explore the model of bovine pulmonary artery EC (BPAEC) infected with constitutively activated ALK1 and ALK5. This model was previously used in several studies designed to elucidate the distinct role of ALK1 and ALK5 receptors in the regulation of EC function (Goumans et al., 2003b; Ota et al., 2002). Importantly, this model mimics, in part, the conditions of chronic inflammation in the lung. We consider that this molecular approach is an appropriate model to study the specific role of distinct TGF-β1 receptors in the activation of signaling pathways controlling endothelial barrier function. Binding of TGF-β1 to receptors results in down-regulation of TGF-β1-induced signaling. Receptors undergo recycling in both the presence and absence of ligand activation, with the rates of internalization and recycling being unaffected by ligand binding. Activated TGF-β1 receptors are directed to a distinct endocytic pathway for down-regulation (Mitchell et al., 2004). The ubiquitin-proteasome pathway, an evolutionarily conserved cascade, tightly regulates TGF-β1 family signaling (Fukunaga et al., 2008; Inoue and Imamura, 2008; Itoh and ten Dijke, 2007; Izzi and Attisano, 2004). TGF-β1 binding to its receptors initiates the degradation of several key components of its signaling pathway. Inhibition of the proteasome activity causes accumulation of these components in cells and modulates TGF-β signaling in a time-dependent and gene-specific manner (Zhang and Laiho, 2003). It is known that under pro-inflammatory conditions ubiquitinated aggregates can accumulate in cells as detergent- resistant aggregates localized in the cytoskeletal compartment (Ogburn

and Figueiredo-Pereira, 2006). It was suggested that receptor ubiquitination and proteasome degradation is the feedback mechanism responsible for physiological responses to stressful stimulation (Ciechanover, 1994; Finley et al., 2004).

The 90-kDa heat-shock protein (Hsp90) is an abundant molecular chaperone that functions by facililitating protein folding and stabilization (Picard, 2002; Pratt and Toft, 2003; Wrighton et al., 2008; Zhang and Burrows, 2004). Pharmacological inhibition of Hsp90 results in ubiquitin-mediated degradation of client proteins (Kamal et al., 2003; Zhang and Burrows, 2004). Heat shock protein 27 (Hsp27) is a well-known Hsp90 client protein (Antonov et al., 2008; Kindas-Mugge et al., 2002). It binds to actin and, when phosphorylated in the cytoskeleton, promotes actin-myosin association (Bitar, 2002; Huot et al., 1996; Mounier and Arrigo, 2002; Piotrowicz et al., 1998). Phosphorylated Hsp27 mediates Rho-induced MYPT1 (myosin phosphatase target subunit 1) phosphorylation and cellular contraction, leading to the increases in EC permeability (Bogatcheva et al., 2007). Cytokines such as TNF and IL-1 can induce Hsp27 phosphorylation, which is linked with edemic effects of these cytokines. Recently, we have demonstrated that TGF-β1-induced hyperpermeability of EC monolayer is associated with increases of Hsp27 phosphorylation and Hsp90-Hsp27 complex formation (Antonov et al., 2008). These data raised the possibility that translocation of Hsp27 into the cytoskeleton that is induced by activated TGF-β1 receptors and its phosphorylation play a role in controlling EC permeability. Hsp27 is required for cell survival and is thought to be involved in protein chaperone function in the cell (Jakob et al., 1993). Hsp27 binds to and inactivates the pro-apoptotic molecules Smac, caspase 3, caspase 9, and cytochrome c release (Pandey et al., 2000). Hsp27 expression and phosphorylation directly affects EC cytoskeleton arrangement and parallels the increase in EC permeability (Antonov et al., 2008). Apoptosis is a potential mechanism associated with phosphorylated Hsp27 translocation in the cytoskeleton compartment and EC hyperpermeability.

We hypothesized that the predominant translocation of ALK5 receptor into the cytoskeleton and its ubiquitination is the principal mechanism leading to the divergence of signals induced by ALK1 and ALK5 receptors. We demonstrate that ALK1 and ALK5 are associated with Hsp90 and that the Hsp90 inhibitor radicicol (RA) protects from the disregulation of endothelial barrier function induced by constitutively active ALK5 (caALK5) infection. These findings uncover the novel mechanism of regulation of endothelial barrier function by TGF-β1 receptors, which includes activation of Hsp90-mediated EC signaling pathways and supports the possibility that Hsp90 inhibitors (some of which are in clinical cancer trials) may have therapeutic value in the improvement of ALI and ARDS.

Materials and Methods

Antibodies and reagents

Primary antibodies were obtained as follows: anti-β-Catenin mAb were from ZYMED Laboratories (South San Francisco, CA). Anti- phospho-hsp27 (Ser 82), anti-VE-cadherin, anti-diphospho-MLC (Thr18/Ser19) polyclonal and anti-phospho-p38MAPK (Thr180/Tyr182) antibodies (Abs) were from Cell Signaling Technology, Inc. (Danvers, MA). Anti-Hsp27 polyclonal antibody (Ab) was from Stressgen Bioreagents Corporation (Ann Arbor, MI). Anti- PARP (poly(ADP-ribose) polymerase) polyclonal Ab, anti-green fluorescent protein (GFP), anti-β-Tubulin and anti-Ubiquitin (P4G7) mAbs were from Covance, Inc. (Emeryville, CA). Anti-β-actin, anti-MLC mAbs and tetramethylrhodamine isothiocynate (TRITC)-conjugated phalloidin were from Sigma-Aldrich (St. Louis, MO). Anti-ALK1 (ACVRL1, N-term) polyclonal Ab was purchased from Abgent (San Diego, CA). Anti-phospho-Caldesmon (p-CaD) (Ser789), anti-ALK5 (V-22) polyclonal Abs and HA-probe

(F-7) mAb were from Santa Cruz Biotechnology (Santa Cruz, CA). Anti-Hsp90 and anti-L-Caldesmon (CaD) mAbs were from BD Transduction Laboratories (Bedford, MA). Alexa Fluor 488 conjugated secondary Ab and ProLong Gold antifade reagent (mounting medium) with and without DAPI were purchased from Molecular Probes (Eugene, OR). ALK5 inhibitor SB-431542 was obtained from Tocris (Ellisville, MO). Selective inhibitor of Rho-associated protein kinase Y-27632, selective inhibitor of p38MAPK SB-203580, Protein G Plus/Protein A Agarose Suspension and ProteoExtract Subcellular Proteome Extraction Kit were from Calbiochem (Merck KGaA, Darmstadt, Germany). Rac G-LISA Activation Assay Biochem kit was from Cytoskeleton (Denver, CO). Unless specified, biochemical reagents were obtained from Sigma-Aldrich (St. Louis, MO).

Construction of recombinant adenoviruses

Recombinant adenoviruses were constructed as described by (Fujii et al., 1999). Briefly, hemagglutinin (HA)-tagged type 1 receptor caALK1 or caALK5 was subcloned into the Swa*I* site of the pAxCAwt cassette cosmid. Each cosmid carrying the expression unit and adenovirus DNA-terminal protein complex were cotransfected into E1 transcomplemental cell line 293. The recombinant adenoviruses generated by homologous recombination were isolated, and the insertion of type 1 receptor cDNAs was confirmed by digestion using restriction endonucleases. Thus, caALK1 and caALK5 generated by the recombinant adenovirus contain an HA- tag and can be detected by HA-tag-specific antibody. High-titered stocks of recombinant adenoviruses were grown in 293 cells and purified. Recombinant adenoviruses with the insertion of GFP cDNAs (Ad5-CMV-GFP) were purchased from Vector Development Laboratory (Houston, TX).

Cell culture and adenoviral infection

We utilized in-house harvested BPAEC, which we have previously characterized extensively for different models (Antonov et al., 2008; Chatterjee et al., 2008). Cultures were maintained in medium 199, supplemented with 10% fetal bovine serum, 5% iron-supplemented calf serum (HyClone, Logan, Ut), 2mM L-glutamine, 1mM sodium pyruvate, 100U/ml penicillin, 100 μg/ml streptomycin (all from Invitrogen, San Francisco, CA). In all experiments BPAEC monolayers (passages 4-10) were used 4-6 day after seeding. BPAEC were infected with HA-tagged caALK1 or caALK5 adenoviral constructs at multiplicity of infection (m.o.i.) of 10-50 pfu/cell for 18 hrs. Cells were washed and allowed to recover for 24 hrs prior to use. Recombinant adenoviruses with the insertion of GFP cDNAs (Ad5-CMV-GFP) were used as a control.

Endothelial monolayer permeability assay

Changes in endothelial permeability were assessed by measuring electrical resistance across monolayer (TER) using the electrical cell impedance sensor technique (Applied Biophysics, Troy, NY), as previously described (Antonov et al., 2008; Antonova et al., 2007b; Birukova et al., 2005b; Verin et al., 2001). Briefly, equivalent numbers of endothelial cells were plated on gold electrode arrays (8W10E) and experiments were conducted after BPAEC formed confluent monolayers (TER had achieved 1000-1200Ω). Cells were then treated as described, and TER was recorded over time.

Immunofluorescense microscopy

Immunofluorescense microscopy studies were performed as we have previously described (Antonov et al., 2008; Birukova et al., 2004; Verin et al., 2001). After treatment BPAEC grown on coverslips were washed with PBS three times, fixed in 3.7% paraformaldehyde for 10 min, and permeabilized with 0.2% Triton X-100 for 10 min. Cells were blocked with PBS-Tween 20 containing 2% BSA for 30 min and incubated with primary antibodies 1h at

37°. Specimens were washed and exposed to Alexa Fluor 488 conjugated secondary antibodies 1h at room temperature. Actin was visualized by TRITC-labeled phalloidin (1mM in PBS, with 0.1% BSA) placed onto the coverslips for 30 min. Coverslips were mounted with ProLong Gold antifade mounting medium (Molecular Probes, Eugene, OR). To detect chromatin condensation, slides were mounted in ProLong Gold antifade mounting medium with DAPI. Specimens were analyzed under a ZEISS Axio Imager Observer D1 epifluorescence microscope.

Western immunoblotting and co-immunoprecipitation

After treatments, BPAEC monolayers were rinsed with PBS, lysed with 2×SDS sample buffer, and boiled for 5 min. Extracts were separated on SDS-PAGE, transferred to PVDF or nitrocellulose membranes and reacted with the antibody of interest. Immunoreactive proteins were visualized with enhanced chemiluminescent detection system (Amersham, Little Chalfont, UK). The relative intensities of the proteins bands were quantified by scanning densitometry using National Institute of Health's ImageJ software (Bethesda, MD). For immunoprecipitation, cells were lysed with ice-cold immunoprecipitation buffer (20 mM Tris HCl, pH 7.4; 137 mM NaCl; 10% glycerol; 1% Nonidet P-40; 2 mM EDTA; 1 mM Na_3VO_4; 20 mM Na_2MoO_4; 1mM NaF; and protease inhibitor cocktail), sonicated 3 times for 15 seconds. The cell lysates were clarified by centrifugation at 12,000 × *g* for 10 min at 4 °C, and the protein concentrations were determined with a BCA protein assay reagent kit as described by the manufacturer (Pierce, Thermo Fisher Scientific, Rockford, IL Pierce). The supernatant was immunoprecipitated with anti-HA-tag Ab (5 μg/ml) overnight at 4°C followed by incubation with protein G plus agarose beads for 4 hrs at 4°C. Agarose beads were collected by centrifugation, washed three times with PBS, resuspended in 40-60 μl of 3×SDS sample buffer, then boiled for 5 min. Protein was separated on 4-12% gradient SDS-PAGE. The resulting membranes were blotted with Hsp90, ubiquitin or HA-tag Abs.

Preparation of subcellular fractions

After treatment BPAEC were rinsed with PBS and used for differential extraction of proteins from subcellular fractions (cytosol, membrane/organelle, nucleus, cytoskeleton) using the Calbiochem ProteoExtract Subcellular Proteome Extraction Kit (S-PEK) (Merck KGaA, Darmstadt, Germany) according to the manufacturer's protocol. Protein in the subcellular fractions was measured using BCA assay kit (Pierce, Thermo Fisher Scientific, Rockford, IL). Protein concentration was equalized between samples in each fraction. For Western blotting 6×SDS sample buffer was added to each sample and boiled for 5 min. Immunoblotting analysis was performed as described above. For co-immunoprecipitation experiments, 50 μg protein of the cytoskeletal fraction in 250 μl of the corresponding buffer from the kit were used. All steps of co-immunoprecipitation and following Western blot analysis were performed as described above for whole cell lysates.

Rac activation assay

BPAEC cultured for 5 days in 35-mm dishes were infected with caALK1, caALK5 (50 m.o.i.) or GFP constructions for 42 hrs. For measurement of Rac 1 activation, the Rac G-LISA Activation Assay Biochem kit (Cytoskeleton, Denver, CO) was used according to the manufacturer's recommendations. The Rac activation signal measured by G-LISA was presented as absorbance at 490 nm.

Statistical analysis

Values are reported as mean ± SE. Comparisons between control and treated cells were performed utilizing t-test or one-way ANOVA, as appropriate, using GraphPad InStat 3.0 software (San Diego, CA). Differences of $p \leq 0.05$ were considered significant.

Results

Time- and dose-dependent expression of TGF-β receptors induced by infection of BPAEC with caALK1 and caALK5 adenoviral constructs

We initially determined the optimal caALK1 and caALK5 adenoviral concentrations and exposure times that result in significant production of the corresponding activated receptors. We found that exposure for 42 hrs with both caALK1 and caALK5 constructs results in a significant production of caALK1 and caALK5 receptors in a dose-dependent manner (Fig. 1A) revealed by Western blot with anti-HA-tag specific antibody. Optimal concentration for caALK1 and caALK5 stimulation was 20-50 m.o.i. After 18 and 42 hrs of treatment with both adenoviral constructs (50 m.o.i.) significant accumulation of both receptors in BPAEC was observed (Fig. 1B). Expression of caALK1 and caALK5 could also be detected as early as 8 hrs after infection with longer exposure times (data not shown). To determine the specifity of infection, we examined the products induced by caALK1 and caALK5 adenoviral infection using antibodies specific to ALK1 and ALK5 receptors. We found that infection with caALK5 results in the expression of only ALK5 receptor. Similarly, caALK1 infection activates synthesis of only ALK1 receptor (Fig. 1C). Next, we addressed the question whether caALK1 or caALK5 infection can induce significant accumulation of the corresponding receptors only in a specific population of BPAEC or in the majority of BPAEC. We found that infection with both adenoviral constructs results in caALK5 and caALK5 receptor expression more than in 95% of BPAEC (Fig. 1D). Thus, we concluded that adenoviral infection with caALK1 and caALK5 adenoviral constructs results in specific and significant production of active receptors in BPAEC.

Effect of caALK1 and caALK5 adenoviral infection on BPAEC permeability

To test the hypothesis that caALK1 and caALK5 expression results in EC permeability changes we examined the effect of caALK1 and caALK5 adenoviral infection on changes in BPAEC TER, which inversely correlates with changes in endothelial permeability (Keese et al., 2004; Verin et al., 2001). We found that caALK1 infection has a minor effect on the BPAEC TER (Fig. 2A). Only a high concentration of caALK1 (50 m.o.i.) induces a decline in BPAEC TER (15-20%). In contrast, caALK5 infection results in significant increases of BPAEC permeability at all caALK5 concentrations tested (Fig. 2B). The changes in BPAEC TER can be detected as early as 6-8 hrs after infection suggesting that even the relatively low amounts of caALK5 receptor expressed soon after infection are sufficient to alter BPAEC permeability. Next, we found that an inhibitor of ALK5 receptor activity, SB-431542 (10-40 μM) completely abolishes the effect of caALK5 on BPAEC TER, but has no effect on the changes in TER induced by caALK1 infection (Fig. 2C, D). Additionally we found that the Rho kinase inhibitor, Y27632 (10 μM) and p38MAPK inhibitor, SB203580 (20 μM) significantly attenuated the effect of caALK5 infection on BPAEC permeability (Supplemental Fig. 1), suggesting that Rho and p38MAPK pathways are involved in ALK5-induced permeability. However, inhibition of Rho and p38MAPK signaling is not sufficient to abolish the effect of ALK5 on EC permeability changes. These data suggest that caALK5 compared to caALK1 is a more a prominent and highly specific activator of the signaling pathways involved in controlling endothelial permeability.

Infection with caALK5 results in the loss of BPAEC integrity via the mechanisms requiring BPAEC cytoskeleton rearrangement

We compared the morphological changes in BPAEC monolayers induced by caALK1 and caALK5 infection and found that caALK5, but not caALK1 or GFP infection, induces a clearly visible BPAEC detachment and the loss of monolayer integrity (Fig. 3A, B, C). To determine whether these changes in monolayer integrity are mediated via cytoskeleton rearrangement, we examined F-actin and β-tubulin organization after caALK1 and caALK5

infection. Treatment with caALK1 (50 m.o.i.; 18 hrs) has a minor effect on cortical F-actin structure and stress fiber formation as well as on β-tubulin arrangement (Fig. 3E, H) as compared with control BPAEC infected with a GFP adenoviral construct (Fig. 3D, G). In contrast, infection with caALK5 results in a dramatic rearrangement of both F-actin and peripheral β-tubulin (Fig. 3F, I). Treatment with caALK5 at 10-20 m.o.i for 18 hrs stimulates stress fiber formation, disruption of cortical actin and leads to gap formation between cells, suggesting endothelial cell contraction. Moreover, the involvement of F-actin in caALK5-induced EC cytoskeletal rearrangement was supported by the inhibition of Rho GTPase Rac1(Supplemental Fig. 2A), which is directly linked to stabilization of cortical actin and EC barrier enhancement (Bogatcheva et al., 2007; Clements et al., 2005; Spindler et al.; Tapon and Hall, 1997). Finally, we find that caALK5 infection results in decreased β-catenin and VE-cadherin expression (Supplemental Fig. 2B), in the BPAEC cytoskeleton fraction, which is known to be important for tight junction formation between endothelial cells and in maintaining endothelial barrier function (Di et al., 2007; Hurst et al., 1999; Rudini et al., 2008).

Adenoviral infection with caALK5 induced BPAEC apoptosis

As demonstrated in Figure 3C, caALK5 overexpression results in significant BPAEC detachment suggesting that caALK5 may have an effect on the contact of BPAEC with substrate. The contact of EC with extracellular matrix is essential for cell survival. Infection of BPAEC with the caALK5 constructs compared to infection with caALK1 results in increased numbers of cells (up to 40%) that show chromatin condensation and nuclear fragmentation revealed by DAPI staining (Fig. 4A, B), indicating EC apoptosis (Antonova et al., 2007b; Martin and Green, 1995; Mills et al., 1999). Additionally, caALK5 but not caALK1 infection increases the level of cleaved PARP (inactive PARP) and decreased the level of active PARP (Fig. 4C, D, E), which is known to be important in the repair of damaged DNA and thus is considered to be characteristic of active cell apoptosis (Martin and Green, 1995; Oliver et al., 1998).

Effect of caALK1 and caALK5 infection on myosin light chain and caldesmon phosphorylation

Key endothelial contractile events in several models of agonist-induced barrier dysfunction are the phosphorylation of regulatory myosin light chain (MLC) and caldesmon, actin and myosin-binding regulatory protein (Bogatcheva and Verin, 2009; Garcia et al., 1995; Garcia and Schaphorst, 1995; Verin et al., 2001; Verin et al., 1998; Verin et al., 1995). Thus we examined the effects of caALK1 and caALK5 adenoviral infection on MLC and caldesmon phosphorylation. We found that treatment with the caALK1 adenoviral construct had no significant effect on MLC or caldesmon phosphorylation (Fig. 5) whereas caALK5 infection results in 2-3 fold increase in diphospho-MLC and 5-fold phospho-caldesmon levels (Fig. 5) after 18 hrs of exposure with adenoviral constructs. These data indicate that caALK5 specifically targets key EC contractile pathways.

Effect of caALK1 and caALK5 infection on Hsp27 and phosphorylated Hsp27 levels in cytosolic and cytoskeletal fractions of BPAEC

Phosphorylation of Hsp27 is directly linked with stabilization of F-actin (Huot et al., 1997; Huot et al., 1998; Huot et al., 1996; Hurst et al., 1999) and is involved in the regulation of EC permeability induced by TGF-β (Antonov et al., 2008; Di et al., 2007).

We examined the effect of caALK1 and caALK5 adenoviral infection on the levels of phosphorylated Hsp27 and total Hsp27 in cytosolic and cytoskeletal compartments of BPAEC. We have found that in cytosol both caALK1 and caALK5 infections significantly increased the level of the phospho-Hsp27 (Fig. 6A) but not total Hsp27. Indeed, in cytosol,

the level of phospho-Hsp27 induced by caALK1 infection was significantly (more than 2 times) higher then after caALK5 infection (Fig, 6B). In cytoskeleton we have found total and phospho-Hsp27 expression only in the samples subjected to caALK1 or caALK5 infections (Fig, 6C). In contrast with cytosol, the level of phospho-Hsp27 induced by caALK5 infection in cytoskeleton fraction was significantly (more than 3 times) higher than after caALK1 infection (Fig, 6D). The ratio of phospho-Hsp27/Hsp27, calculated as fold increase to caALK1 (Fig. 6E), revealed that after caALK5 infection the level of phosphorylated Hsp27 in cytoskeleton significantly increased compared with that in cytosol.

These data suggest that caALK5 induction of specific translocation of phosphorylated Hsp27 in the cytoskeletal compartment could be the mechanism driving the distinct responses of BPAEC to constitutively activated TGF-β receptors.

caALK1 and caALK5 receptors interact with Hsp90

We hypothesized that Hsp90 is associated with ALK1 and ALK5 receptors. To test this hypothesis, BPAEC were infected with adenoviral constructs and whole cell lysates immunoprecipitated with anti-HA-tag mAb. We then examined the expression of Hsp90 in the immunoprecipitates with Hsp90-specific mAb. As shown in Figure 7A, immunoprecipitation with anti-HA-tag mAb reveals significant expression of Hsp90 after infection with both caALK1 and caALK5. It has been shown that release of client proteins from Hsp90 complexes results in their ubiquitination and degradation (Kamal et al., 2003; Picard, 2002; Zhang and Burrows, 2004). We thus addressed the question whether caALK1 and caALK5 produced via adenoviral infection are ubiquitinated. We have found that the gene products immunoprecipitated with anti-HA-tag Ab after caALK5 infection are ubiqutinated (Fig. 7B), whereas immunoprecipitates following caALK1 infection were not ubiquitinated. Western blot analysis of proteins from whole cell lysate (Fig. 7C) separated by SDS-PAGE revealed equal expression of HA-tagged ALK1 and ALK5. Expression of GFP used as a control. β-actin level examined to verify equal protein loading.

Specific accumulation of ubiqutinated caALK5 receptor in the BPAEC cytoskeletal compartment

We demonstrated that caALK5 adenoviral infection results in the predominant translocation of Hsp27 into BPAEC cytoskeleton (Fig. 6). Hsp90 is associated with both Hsp27 (Kindas-Mugge et al., 2002) and TGF-β1 receptors (Wrighton et al., 2008). We have shown that both, caALK5 and caALK1 are Hsp90 client proteins, but only caALK5 is ubiquitinated (Fig. 7). We hypothesized that caALK5 also translocates into BPAEC cytoskeletal compartment. To test this, we examined caALK1 and caALK5 accumulation in subcellular fractions after adenoviral infection. As shown in Figure 8A, caALK1 and caALK5 have comparable levels of expression in the membrane/organelle and nuclear fractions. Surprisingly, in contrast with caALK1, caALK5 infection results in a large accumulation of caALK5 in the cytoskeletal fraction as revealed by Western blotting with HA-tag-specific Ab. Microtubule dissolution and F-actin rearrangement parallel accumulation of ubiquitinated protein in the detergent insoluble (cytoskeleton) fraction (Ogburn and Figueiredo-Pereira, 2006). Thus, we examined whether caALK5 expressed in the BPAEC cytoskeleton is ubiquitinated. We find that only caALK5 located in the cytoskeleton is ubiquitinated (Fig. 8C). This mechanism may be of importance in the regulation of BPAEC permeability.

Hsp90 inhibitor RA prevents hyperpermeability induced by caALK5 adenoviral infection via a mechanism requiring inhibition of ubiquitinated caALK5 and phospho-Hsp27 accumulation in the cytoskeletal fraction

Hypothetically, Hsp90 inhibitors may attenuate the effects of caALK5 and improve BPAEC barrier function. We found that the Hsp90 inhibitor RA (1 μM) completely abolished translocation of caALK5 into cytoskeleton and expression of ubiquitinated proteins (Fig. 9A, B) revealed by Western blotting analysis with HA-tag or ubiquitin-specific Abs. To test the hypothesis that proteasome-dependent mechanisms are involved in these effects, we treated cells with the proteasome inhibitor lactacystin (LA, 5 μM) in the presence or absence of RA. We found that RA abolished accumulation of ubiquitinated proteins in the cytoskeleton induced by caALK5 infection, whereas LA restored expression of ubiquitinated proteins (Fig. 9C). Re-probing the blot with HA-tag Ab together with the data presented in Figure 7 suggested that the ubiquitinated protein is ALK5. To prove that the ubiquitinated protein indeed is ALK5, we immunoprecipitated the cytoskeletal fraction with HA-tag Ab and examined the effect of RA and LA specifically on caALK5 expression and ubiquitination with HA-tag and ubiquitin Abs (Fig. 9D). We found that RA abolished the increases of ubiquitinated caALK5 expression in the cytoskeleton. As predicted, LA increased the accumulation of ubiquitinated caALK5 in the cytoskeleton. This effect of LA in the presence of RA was minimal (Fig. 9D), suggesting that RA may activate proteasome-independent mechanisms of ubiquitinated protein degradation, for example, by lysosomes. These data suggest that proteasome degradation of ALK5 plays a role in the effects of RA on EC permeability. Next we demonstrated that RA completely prevents the decline in TER induced by exposure with caALK5 adenoviral constructs (Fig. 9E). Finally, we demonstrated that RA treatment decreased phospho-Hsp27 expression in the cytoskeleton induced by caALK5 adenoviral infection (Fig. 9F). Surprisingly, caALK1 adenoviral infection in the presence of RA increased phospho-Hsp27 expression in the BPAEC cytoskeleton as compared with GFP infection, whereas RA alone has no effect on the phospho-Hap27 level. Currently, we do not have an explanation of the molecular mechanisms of the synergistic effects of RA and caALK1 infection on phospho-Hsp27-regulated signaling pathways.

Discussion

In the present study, we demonstrate for the first time that the roles of ALK1 and ALK5 in the regulation of EC barrier dysfunction are not identical. We hypothesize that specific translocation of ALK5 receptor into the cytoskeleton and its ubiquitination is the checkpoint where the signal transduction pathways activated by ALK1 and ALK5 diverge. Our data demonstrate the role of ubiquitin and the proteasome in the regulation of TGF-β1 signaling and establish an important role of Hsp90 and Hsp27 in controlling endothelial barrier functions. Finally, our data raise the possibility that inhibitors of Hsp90 may improve inflammatory status in the lung by preventing endothelial dysfunction induced by sustained activation of ALK5.

Initially, we intended to document that caALK1 and caALK5 adenoviral infections indeed have different effects on endothelial permeability and integrity. Multiple signaling pathways, including SMAD-dependent and independent mechanisms, were described by us and others (Birukova et al., 2005a; Finnson et al., 2008; Goumans et al., 2003a; Goumans et al., 2003b; Goumans et al., 2002; Itoh and ten Dijke, 2007; Lebrin et al., 2004; Lu et al., 2006). In this study, we focus only on the several pathways known to be critical in the control of endothelial permeability induced by TGF-β1 activation, which obligatorily leads to endothelial barrier dysfunction (Birukova et al., 2005a; Lebrin et al., 2005; Pittet et al., 2001). We demonstrate that infection with caALK5, in contrast with caALK1, activates MLC and caldesmon and stimulates phosphorylated Hsp27 translocation into the

cytoskeletal fraction. We find that only caALK5, but not caALK1, results in F-actin stress fiber formation as well as disruption of the peripheral microtubules meshwork and gap formation between EC. We also find that caALK5 infection results in a significant decrease in VE-cadherin and β-catenin expression in the BPAEC cytoskeleton, which is important for formation of appropriate contacts (tight junctions) between EC, suggesting that exposure to caALK5 disrupts endothelial monolayer organization. These data directly indicate specific activation of EC contractile mechanisms by sustained activated ALK5.

In this study, we have found that caALK5 activates apoptosis in EC. It is well known that the loss of contact of EC with substrates leads to EC apoptosis (Mills et al., 1999). Our data imply that caALK5 infection also targets contact of EC with the extracellular matrix. Probably the differences between TGF-β1 stimulation and sustained activation of ALK5 depend on the duration of stimuli and activation of feedback mechanisms that allow EC to escape from an activated state. Also, it is possible that the differences in EC permeability induced by caALK1 and caALK5 are mediated by the induction of EC detachment and apoptosis by caALK5 treatment.

The major goal of this study was to identify the regulatory checkpoints where contractile signaling pathways initiated by caALK1 and caALK5 diverge. We focused on two events directly associated with regulation of EC barrier function, namely, effects of caALK1 and caALK5 adenovirus infections on phospho-Hsp27 and caALK5 distribution in different subcellular compartments. Phosphorylated Hsp27 is an F-actin stabilizing protein (Bitar, 2002; Huot et al., 1997; Huot et al., 1998; Huot et al., 1996) and plays a role in the regulation of EC cytoskeletal arrangement. Several inflammatory cytokines can induce Hsp27 phosphorylation, which is linked with edemic effects of these cytokines (Antonov et al., 2008; Bertolino et al., 2005; Pittet et al., 2001; Rogalla et al., 1999). Previously we have shown that TGF-β1-induced hyperpermeability is associated with increased Hsp27 phosphorylation, association of Hsp27 with Hsp90, and intensive F-actin stress fiber formation (Antonov et al., 2008). We have also demonstrated that Rho-kinase and p38MAPK are involved in the transduction of signals induced by TGF-β1 (Bogatcheva et al., 2007). We have now demonstrated that the effects of Hsp27 on EC barrier function require accumulation of phospho-Hsp27 specifically in the BPAEC cytoskeleton. An important novel finding is that caALK5 infection results in specific accumulation of the ubiquitinated ALK5 receptor in the cytoskeleton. We hypothesized that caALK5 adenoviral infection induced specific translocation of Hsp27 and ALK5 into the cytoskeleton and that this is the checkpoint where signaling induced by caALK1 and caALK5 diverge.

The strength and duration of TGFβ-1 signaling largely depends on a negative feedback program initiated during signal progression (Itoh and ten Dijke, 2007). Receptor ubiquitination following degradation is one of the critical mechanisms controlling the transition between an active and inactive state in the cells. One of the mechanisms leading to accumulation of ubiquitinated proteins is the lack (or insufficient function) of proteasome degradation. Ubiquitin targets aberrant proteins to degradation by the proteasome/lysosome (Finley et al., 2004). The mechanisms implicated in the formation of aggregates containing ubiquitinated proteins remain unclear. Protein aggregates containing ubiquitinated proteins are detected in a variety of degenerative diseases (Lennox et al., 1988; Lowe et al., 1988a; Lowe et al., 1988b). It has been shown that microtubule collapse parallels deposition of ubiquitinated protein aggregates (Ogburn and Figueiredo-Pereira, 2006). Most ubiquitinated proteins were detected in the Triton X-100 insoluble fraction (cytoskeletal). This aberrant protein deposition, triggered by the products of inflammation, may be common to different compounds that disrupt microtubules and induce protein aggregation. Our data demonstrates that caALK5 accumulated in the cytoskeletal compartment is ubiquitinated, implying that proteasomes play a role in the effects of caALK5.

We do not observe significant ALK1 accumulation in the cytoskeletal fraction, whereas the levels of ALK1 and ALK5 in organelle/membrane and nuclear fractions are comparable. Probably these differences in ALK1 and ALK5 expression reflect the lack of ALK5 degradation whereas ubiquitinated ALK1 is degraded. This hypothesis fits with previous data that demonstrated that TGF-β receptors are targets of ubiquitin-mediated degradation (Ebisawa et al., 2001; Itoh and ten Dijke, 2007; Izzi and Attisano, 2004; Kavsak et al., 2000; Zhang and Laiho, 2003).

Importantly, it was reported (Ogburn and Figueiredo-Pereira, 2006) that ubiquitinated protein deposition triggered by products of inflammation can parallel tubulin meshwork collapse and thus inhibit trafficking of ubiquitinated proteins into the proteasome. This results in formation of a positive loop leading to cytoskeletal collapse. It is possible that changes in the F-actin and tubulin arrangement induced by caALK5 are associated with the lack of ubiquitinated caALK5 degradation.

We conclude that caALK5 infection down-regulates proteasome degradation of ubiqutinated ALK5 receptor, leading to accumulation of ubiquitinated protein in the cytoskeleton, which results in the microtubule meshwork collapse and increases in endothelial permeability. Figure 10 summarizes the hypothetical model of the regulation of EC barrier dysfunction induced by caALK5.

Hsp90 is one of the most abundant cellular proteins, accounting for about 1-2% of total proteins under unstressed conditions (Pratt and Toft, 2003). Recently we demonstrated that Hsp90 inhibitors protect and restore the increased EC permeability induced by several inflammatory cytokines including TGF-β1, suggesting that the Hsp90 chaperone complex is critically involved in the regulation of EC permeability (Antonov et al., 2008; Antonova et al., 2007a; Chatterjee et al., 2007). This complex cycles between an “open” and “closed” state conformation, relative to the distance between the N terminals of Hsp90 homodimer. Hsp90 inhibitors shortcut the cycle and lock the complex in the “open” state, resulting in client protein deactivation, destabilization, and proteasomal degradation (Picard, 2002; Zhang and Burrows, 2004). It was suggested that TGF-β1 receptors are Hsp90-interacting proteins (Wrighton et al., 2008) and thus the Hsp90 plays a role in TGF-β1 signaling via its ability to stabilize TGF-β1 receptor. Inhibiting Hsp90 function leads to ubiquitin-mediated degradation of TGF-β1 receptors (Wrighton et al., 2008). Hsp90 inhibitors may activate the turnover of ubiquitinated caALK5 and thus protect from the disregulation of EC barrier function. Indeed, we find that the specific inhibitor of Hsp90 RA prevents phospho-Hsp27 and caALK5 translocation into the cytoskeleton and decreases the expression of ubiquitinated caALK5 in the cytoskeletal fraction. These effects of RA treatment parallel with the improvement of BPAEC permeability induced by caALK5 infection.

In conclusion, we describe here a novel molecular mechanism involved in the regulation of EC barrier function by TGF-β1 receptors. Coupled with the fact that Hsp90 inhibitors are in clinical trials, our data present the genuine possibility that small molecular inhibitors of Hsp90 may represent a class of drugs for treating inflammatory TGF-β1-related conditions in the lung, directed towards specific mechanisms leading to the pathological state.

Supplementary Material

Refer to Web version on PubMed Central for supplementary material.

Acknowledgments

This research was supported by National Institutes of Health Grants HL 080675 and 067307 to A. D. Verin.

Literature Cited

Antonov A, Snead C, Gorshkov B, Antonova GN, Verin AD, Catravas JD. Heat shock protein 90 inhibitors protect and restore pulmonary endothelial barrier function. Am J Respir Cell Mol Biol. 2008; 39(5):551–559. [PubMed: 18474672]

Antonova G, Lichtenbeld H, Xia T, Chatterjee A, Dimitropoulou C, Catravas JD. Functional significance of hsp90 complexes with NOS and sGC in endothelial cells. Clin Hemorheol Microcirc. 2007a; 37(1-2):19–35. [PubMed: 17641392]

Antonova GN, Snead CM, Antonov AS, Dimitropoulou C, Venema RC, Catravas JD. Nitric oxide preconditioning regulates endothelial monolayer integrity via the heat shock protein 90-soluble guanylate cyclase pathway. Am J Physiol Heart Circ Physiol. 2007b; 292(2):H893–903. [PubMed: 17012359]

Bertolino P, Deckers M, Lebrin F, ten Dijke P. Transforming growth factor-beta signal transduction in angiogenesis and vascular disorders. Chest. 2005; 128(6 Suppl):585S–590S. [PubMed: 16373850]

Birukova AA, Adyshev D, Gorshkov B, Birukov KG, Verin AD. ALK5 and Smad4 are involved in TGF-beta1-induced pulmonary endothelial permeability. FEBS Lett. 2005a; 579(18):4031–4037. [PubMed: 16004987]

Birukova AA, Birukov KG, Adyshev D, Usatyuk P, Natarajan V, Garcia JG, Verin AD. Involvement of microtubules and Rho pathway in TGF-beta1-induced lung vascular barrier dysfunction. J Cell Physiol. 2005b; 204(3):934–947. [PubMed: 15828024]

Birukova AA, Smurova K, Birukov KG, Usatyuk P, Liu F, Kaibuchi K, Ricks-Cord A, Natarajan V, Alieva I, Garcia JG, Verin AD. Microtubule disassembly induces cytoskeletal remodeling and lung vascular barrier dysfunction: role of Rho-dependent mechanisms. J Cell Physiol. 2004; 201(1):55–70. [PubMed: 15281089]

Bitar KN. HSP27 phosphorylation and interaction with actin-myosin in smooth muscle contraction. Am J Physiol Gastrointest Liver Physiol. 2002; 282(5):G894–903. [PubMed: 11960785]

Bogatcheva NV, Adyshev D, Mambetsariev B, Moldobaeva N, Verin AD. Involvement of microtubules, p38, and Rho kinases pathway in 2-methoxyestradiol-induced lung vascular barrier dysfunction. Am J Physiol Lung Cell Mol Physiol. 2007; 292(2):L487–499. [PubMed: 17012370]

Bogatcheva NV, Verin AD. Reprint of “The role of cytoskeleton in the regulation of vascular endothelial barrier function” [Microvascular Research 76 (2008) 202-207]. Microvasc Res. 2009; 77(1):64–69. [PubMed: 19232242]

Chatterjee A, Dimitropoulou C, Drakopanayiotakis F, Antonova G, Snead C, Cannon J, Venema RC, Catravas JD. Heat shock protein 90 inhibitors prolong survival, attenuate inflammation, and reduce lung injury in murine sepsis. Am J Respir Crit Care Med. 2007; 176(7):667–675. [PubMed: 17615388]

Chatterjee A, Snead C, Yetik-Anacak G, Antonova G, Zeng J, Catravas JD. Heat shock protein 90 inhibitors attenuate LPS-induced endothelial hyperpermeability. Am J Physiol Lung Cell Mol Physiol. 2008; 294(4):L755–763. [PubMed: 18245267]

Ciechanover A. The ubiquitin-proteasome proteolytic pathway. Cell. 1994; 79(1):13–21. [PubMed: 7923371]

Clements RT, Minnear FL, Singer HA, Keller RS, Vincent PA. RhoA and Rho-kinase dependent and independent signals mediate TGF-beta-induced pulmonary endothelial cytoskeletal reorganization and permeability. Am J Physiol Lung Cell Mol Physiol. 2005; 288(2):L294–306. [PubMed: 15475381]

Di K, Wong YC, Wang X. Id-1 promotes TGF-beta1-induced cell motility through HSP27 activation and disassembly of adherens junction in prostate epithelial cells. Exp Cell Res. 2007; 313(19): 3983–3999. [PubMed: 17916352]

Dudek SM, Garcia JG. Cytoskeletal regulation of pulmonary vascular permeability. J Appl Physiol. 2001; 91(4):1487–1500. [PubMed: 11568129]

Ebisawa T, Fukuchi M, Murakami G, Chiba T, Tanaka K, Imamura T, Miyazono K. Smurf1 interacts with transforming growth factor-beta type I receptor through Smad7 and induces receptor degradation. J Biol Chem. 2001; 276(16):12477–12480. [PubMed: 11278251]

Finley D, Ciechanover A, Varshavsky A. Ubiquitin as a central cellular regulator. Cell. 2004; 116(2 Suppl):S29–32. 22 p following S32. [PubMed: 15055578]

Finnson KW, Parker WL, ten Dijke P, Thorikay M, Philip A. ALK1 opposes ALK5/Smad3 signaling and expression of extracellular matrix components in human chondrocytes. J Bone Miner Res. 2008; 23(6):896–906. [PubMed: 18333754]

Fujii M, Takeda K, Imamura T, Aoki H, Sampath TK, Enomoto S, Kawabata M, Kato M, Ichijo H, Miyazono K. Roles of bone morphogenetic protein type I receptors and Smad proteins in osteoblast and chondroblast differentiation. Mol Biol Cell. 1999; 10(11):3801–3813. [PubMed: 10564272]

Fukunaga E, Inoue Y, Komiya S, Horiguchi K, Goto K, Saitoh M, Miyazawa K, Koinuma D, Hanyu A, Imamura T. Smurf2 induces ubiquitin-dependent degradation of Smurf1 to prevent migration of breast cancer cells. J Biol Chem. 2008; 283(51):35660–35667. [PubMed: 18927080]

Garcia JG, Davis HW, Patterson CE. Regulation of endothelial cell gap formation and barrier dysfunction: role of myosin light chain phosphorylation. J Cell Physiol. 1995; 163(3):510–522. [PubMed: 7775594]

Garcia JG, Schaphorst KL. Regulation of endothelial cell gap formation and paracellular permeability. J Investig Med. 1995; 43(2):117–126.

Goldberg PL, MacNaughton DE, Clements RT, Minnear FL, Vincent PA. p38 MAPK activation by TGF-beta1 increases MLC phosphorylation and endothelial monolayer permeability. Am J Physiol Lung Cell Mol Physiol. 2002; 282(1):L146–154. [PubMed: 11741826]

Goumans MJ, Lebrin F, Valdimarsdottir G. Controlling the angiogenic switch: a balance between two distinct TGF-β receptor signaling pathways. Trends Cardiovasc Med. 2003a; 13(7):301–307. [PubMed: 14522471]

Goumans MJ, Valdimarsdottir G, Itoh S, Lebrin F, Larsson J, Mummery C, Karlsson S, ten Dijke P. Activin receptor-like kinase (ALK)1 is an antagonistic mediator of lateral TGFbeta/ALK5 signaling. Mol Cell. 2003b; 12(4):817–828. [PubMed: 14580334]

Goumans MJ, Valdimarsdottir G, Itoh S, Rosendahl A, Sideras P, ten Dijke P. Balancing the activation state of the endothelium via two distinct TGF-beta type I receptors. EMBO J. 2002; 21(7):1743–1753. [PubMed: 11927558]

Huot J, Houle F, Marceau F, Landry J. Oxidative stress-induced actin reorganization mediated by the p38 mitogen-activated protein kinase/heat shock protein 27 pathway in vascular endothelial cells. Circ Res. 1997; 80(3):383–392. [PubMed: 9048659]

Huot J, Houle F, Rousseau S, Deschesnes RG, Shah GM, Landry J. SAPK2/p38-dependent F-actin reorganization regulates early membrane blebbing during stress-induced apoptosis. J Cell Biol. 1998; 143(5):1361–1373. [PubMed: 9832563]

Huot J, Houle F, Spitz DR, Landry J. HSP27 phosphorylation-mediated resistance against actin fragmentation and cell death induced by oxidative stress. Cancer Res. 1996; 56(2):273–279. [PubMed: 8542580]

Hurst VI, Goldberg PL, Minnear FL, Heimark RL, Vincent PA. Rearrangement of adherens junctions by transforming growth factor-beta1: role of contraction. Am J Physiol. 1999; 276(4 Pt 1):L582–595. [PubMed: 10198356]

Inoue Y, Imamura T. Regulation of TGF-beta family signaling by E3 ubiquitin ligases. Cancer Sci. 2008; 99(11):2107–2112. [PubMed: 18808420]

Itoh S, ten Dijke P. Negative regulation of TGF-beta receptor/Smad signal transduction. Curr Opin Cell Biol. 2007; 19(2):176–184. [PubMed: 17317136]

Izzi L, Attisano L. Regulation of the TGFbeta signalling pathway by ubiquitin-mediated degradation. Oncogene. 2004; 23(11):2071–2078. [PubMed: 15021894]

Jakob U, Gaestel M, Engel K, Buchner J. Small heat shock proteins are molecular chaperones. J Biol Chem. 1993; 268(3):1517–1520. [PubMed: 8093612]

Kamal A, Thao L, Sensintaffar J, Zhang L, Boehm MF, Fritz LC, Burrows FJ. A high-affinity conformation of Hsp90 confers tumour selectivity on Hsp90 inhibitors. Nature. 2003; 425(6956):407–410. [PubMed: 14508491]

Kavsak P, Rasmussen RK, Causing CG, Bonni S, Zhu H, Thomsen GH, Wrana JL. Smad7 binds to Smurf2 to form an E3 ubiquitin ligase that targets the TGF beta receptor for degradation. Mol Cell. 2000; 6(6):1365–1375. [PubMed: 11163210]

Keese CR, Wegener J, Walker SR, Giaever I. Electrical wound-healing assay for cells in vitro. Proc Natl Acad Sci U S A. 2004; 101(6):1554–1559. [PubMed: 14747654]

Kindas-Mugge I, Rieder C, Frohlich I, Micksche M, Trautinger F. Characterization of proteins associated with heat shock protein hsp27 in the squamous cell carcinoma cell line A431. Cell Biol Int. 2002; 26(1):109–116. [PubMed: 11779227]

Lebrin F, Deckers M, Bertolino P, Ten Dijke P. TGF-beta receptor function in the endothelium. Cardiovasc Res. 2005; 65(3):599–608. [PubMed: 15664386]

Lebrin F, Goumans MJ, Jonker L, Carvalho RL, Valdimarsdottir G, Thorikay M, Mummery C, Arthur HM, ten Dijke P. Endoglin promotes endothelial cell proliferation and TGF-beta/ALK1 signal transduction. EMBO J. 2004; 23(20):4018–4028. [PubMed: 15385967]

Lennox G, Lowe J, Morrell K, Landon M, Mayer RJ. Ubiquitin is a component of neurofibrillary tangles in a variety of neurodegenerative diseases. Neurosci Lett. 1988; 94(1-2):211–217. [PubMed: 2853854]

Lowe J, Blanchard A, Morrell K, Lennox G, Reynolds L, Billett M, Landon M, Mayer RJ. Ubiquitin is a common factor in intermediate filament inclusion bodies of diverse type in man, including those of Parkinson's disease, Pick's disease, and Alzheimer's disease, as well as Rosenthal fibres in cerebellar astrocytomas, cytoplasmic bodies in muscle, and mallory bodies in alcoholic liver disease. J Pathol. 1988a; 155(1):9–15. [PubMed: 2837558]

Lowe J, Lennox G, Jefferson D, Morrell K, McQuire D, Gray T, Landon M, Doherty FJ, Mayer RJ. A filamentous inclusion body within anterior horn neurones in motor neurone disease defined by immunocytochemical localisation of ubiquitin. Neurosci Lett. 1988b; 94(1-2):203–210. [PubMed: 2853853]

Lu Q, Harrington EO, Jackson H, Morin N, Shannon C, Rounds S. Transforming growth factor-beta1-induced endothelial barrier dysfunction involves Smad2-dependent p38 activation and subsequent RhoA activation. J Appl Physiol. 2006; 101(2):375–384. [PubMed: 16645187]

Lucas R, Verin AD, Black SM, Catravas JD. Regulators of endothelial and epithelial barrier integrity and function in acute lung injury. Biochem Pharmacol. 2009; 77(12):1763–1772. [PubMed: 19428331]

Martin C, Papazian L, Payan MJ, Saux P, Gouin F. Pulmonary fibrosis correlates with outcome in adult respiratory distress syndrome. A study in mechanically ventilated patients. Chest. 1995; 107(1):196–200. [PubMed: 7813276]

Martin SJ, Green DR. Apoptosis and cancer: the failure of controls on cell death and cell survival. Crit Rev Oncol Hematol. 1995; 18(2):137–153. [PubMed: 7695828]

Mills JC, Stone NL, Pittman RN. Extranuclear apoptosis. The role of the cytoplasm in the execution phase. J Cell Biol. 1999; 146(4):703–708. [PubMed: 10459006]

Mitchell H, Choudhury A, Pagano RE, Leof EB. Ligand-dependent and -independent transforming growth factor-beta receptor recycling regulated by clathrin-mediated endocytosis and Rab11. Mol Biol Cell. 2004; 15(9):4166–4178. [PubMed: 15229286]

Mounier N, Arrigo AP. Actin cytoskeleton and small heat shock proteins: how do they interact? Cell Stress Chaperones. 2002; 7(2):167–176. [PubMed: 12380684]

Ogburn KD, Figueiredo-Pereira ME. Cytoskeleton/endoplasmic reticulum collapse induced by prostaglandin J2 parallels centrosomal deposition of ubiquitinated protein aggregates. J Biol Chem. 2006; 281(32):23274–23284. [PubMed: 16774923]

Oliver FJ, de la Rubia G, Rolli V, Ruiz-Ruiz MC, de Murcia G, Murcia JM. Importance of poly(ADP-ribose) polymerase and its cleavage in apoptosis. Lesson from an uncleavable mutant. J Biol Chem. 1998; 273(50):33533–33539. [PubMed: 9837934]

Ota T, Fujii M, Sugizaki T, Ishii M, Miyazawa K, Aburatani H, Miyazono K. Targets of transcriptional regulation by two distinct type I receptors for transforming growth factor-beta in human umbilical vein endothelial cells. J Cell Physiol. 2002; 193(3):299–318. [PubMed: 12384983]

Pandey P, Farber R, Nakazawa A, Kumar S, Bharti A, Nalin C, Weichselbaum R, Kufe D, Kharbanda S. Hsp27 functions as a negative regulator of cytochrome c-dependent activation of procaspase-3. Oncogene. 2000; 19(16):1975–1981. [PubMed: 10803458]

Parsons PE, Worthen GS, Moore EE, Tate RM, Henson PM. The association of circulating endotoxin with the development of the adult respiratory distress syndrome. Am Rev Respir Dis. 1989; 140(2):294–301. [PubMed: 2764364]

Picard D. Heat-shock protein 90, a chaperone for folding and regulation. Cell Mol Life Sci. 2002; 59(10):1640–1648. [PubMed: 12475174]

Piotrowicz RS, Hickey E, Levin EG. Heat shock protein 27 kDa expression and phosphorylation regulates endothelial cell migration. FASEB J. 1998; 12(14):1481–1490. [PubMed: 9806757]

Pittet JF, Griffiths MJ, Geiser T, Kaminski N, Dalton SL, Huang X, Brown LA, Gotwals PJ, Koteliansky VE, Matthay MA, Sheppard D. TGF-beta is a critical mediator of acute lung injury. J Clin Invest. 2001; 107(12):1537–1544. [PubMed: 11413161]

Pratt WB, Toft DO. Regulation of signaling protein function and trafficking by the hsp90/hsp70-based chaperone machinery. Exp Biol Med (Maywood). 2003; 228(2):111–133. [PubMed: 12563018]

Rogalla T, Ehrnsperger M, Preville X, Kotlyarov A, Lutsch G, Ducasse C, Paul C, Wieske M, Arrigo AP, Buchner J, Gaestel M. Regulation of Hsp27 oligomerization, chaperone function, and protective activity against oxidative stress/tumor necrosis factor alpha by phosphorylation. J Biol Chem. 1999; 274(27):18947–18956. [PubMed: 10383393]

Rudini N, Felici A, Giampietro C, Lampugnani M, Corada M, Swirsding K, Garre M, Liebner S, Letarte M, ten Dijke P, Dejana E. VE-cadherin is a critical endothelial regulator of TGF-beta signalling. EMBO J. 2008; 27(7):993–1004. [PubMed: 18337748]

Spindler V, Schlegel N, Waschke J. Role of GTPases in control of microvascular permeability. Cardiovasc Res. 87(2):243–253. [PubMed: 20299335]

Tapon N, Hall A. Rho, Rac and Cdc42 GTPases regulate the organization of the actin cytoskeleton. Curr Opin Cell Biol. 1997; 9(1):86–92. [PubMed: 9013670]

Verin AD, Birukova A, Wang P, Liu F, Becker P, Birukov K, Garcia JG. Microtubule disassembly increases endothelial cell barrier dysfunction: role of MLC phosphorylation. Am J Physiol Lung Cell Mol Physiol. 2001; 281(3):L565–574. [PubMed: 11504682]

Verin AD, Gilbert-McClain LI, Patterson CE, Garcia JG. Biochemical regulation of the nonmuscle myosin light chain kinase isoform in bovine endothelium. Am J Respir Cell Mol Biol. 1998; 19(5): 767–776. [PubMed: 9806741]

Verin AD, Patterson CE, Day MA, Garcia JG. Regulation of endothelial cell gap formation and barrier function by myosin-associated phosphatase activities. Am J Physiol. 1995; 269(1 Pt 1):L99–108. [PubMed: 7631821]

Wrighton KH, Lin X, Feng XH. Critical regulation of TGFβ signaling by Hsp90. Proc Natl Acad Sci U S A. 2008; 105(27):9244–9249. [PubMed: 18591668]

Zhang F, Laiho M. On and off: proteasome and TGF-beta signaling. Exp Cell Res. 2003; 291(2):275–281. [PubMed: 14644150]

Zhang H, Burrows F. Targeting multiple signal transduction pathways through inhibition of Hsp90. J Mol Med. 2004; 82(8):488–499. [PubMed: 15168026]

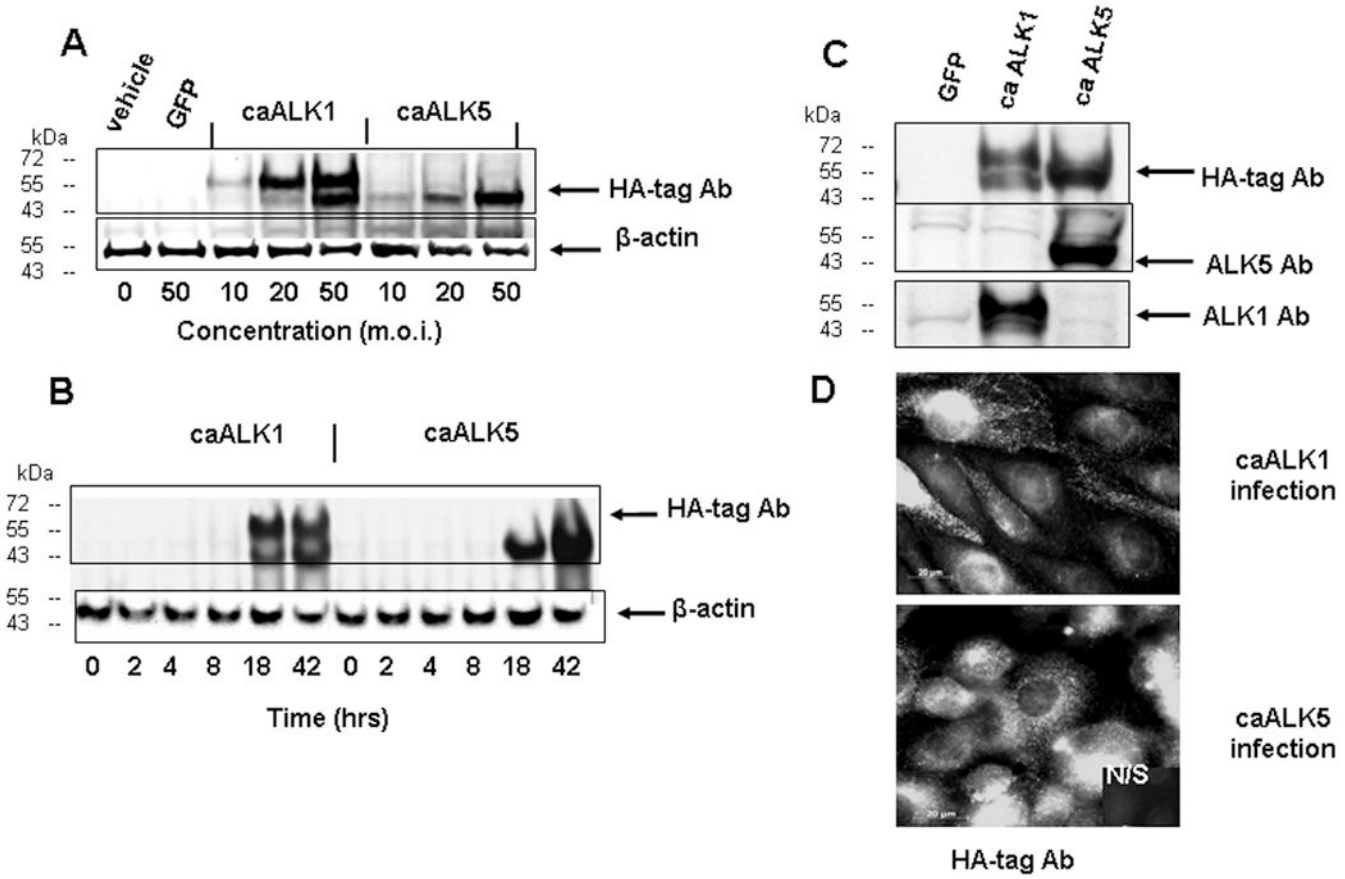

Figure 1. Dose-and time-dependent accumulation of caALK1 and caALK5 in BPAEC

(A) BPAEC were exposed to10-50 m.o.i. of HA-tagged caALK1, HA-tagged caALK5, GFP or vehicle for 42 hrs (n=7). (B) BPAEC were infected with 50 m.o.i. of HA-tagged caALK1 or HA-tagged caALK5 and examined at different time intervals after infection. Control cells were infected with 50 m.o.i. of GFP adenoviral construct or were treated with the vehicle (PBS). Expression of HA-tagged recombinant proteins was detected by Western blotting with HA-tag specific Ab as well as anti-β-actin Ab as loading control. (C) BPAEC were infected with 50 m.o.i. of caALK1 or caALK5 for 42 hrs. Blots were probed with ALK1 and ALK5 specific antibodies (n=5) (D) Immunofluorescent visualization of HA-tagged caALK1 and HA-tagged caALK5 in BPAEC. BPAEC were infected with adenoviral constructs as described in (A) and caALK1 and caALK5 expressions detected with HA-specific Ab (n=4; bars= 20μm; N/S-insert - nonspecific staining)

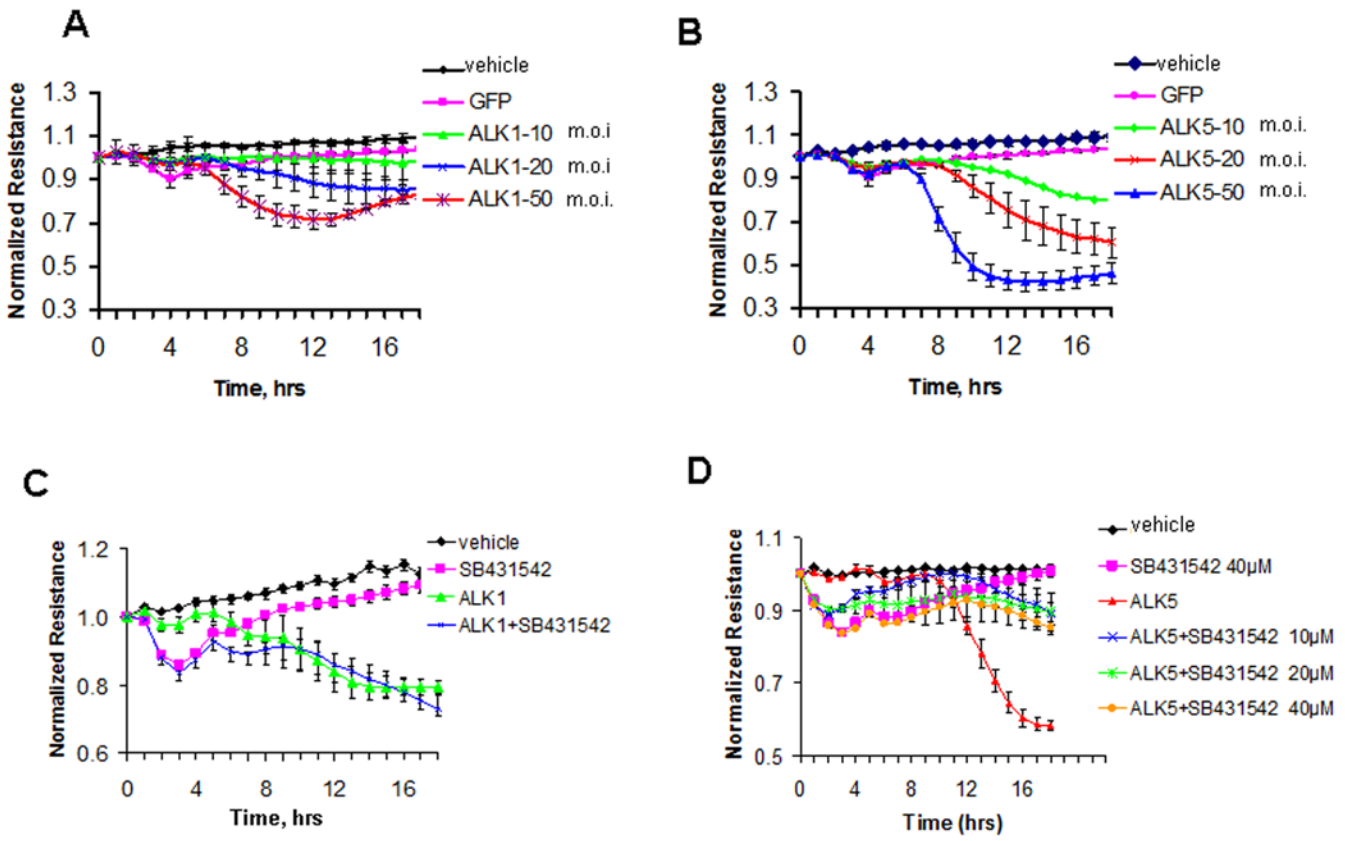

Figure 2. Effect of caALK1 and caALK5 adenoviral infection on BPAEC permeability

BPAEC were plated on gold microelectrodes and cultured for 5 days. (A, B) Cells were infected with caALK1, caALK5, or GFP (all 50 m.o.i.) or treated with vehicle (PBS). TER was measured as an index of the changes in EC permeability (see Methods). Changes in TER were monitored for up to 18 hrs. (C, D) The cells were prepared as described in (A, B), and preincubated with ALK5 inhibitor SB-431542 (10-40μm), or vehicle (0.1% DMSO) for 1 hr and then infected with caALK1, caALK5 (50 m.o.i.). The changes in BPAEC permeability were monitored as described in Methods. (Data are mean±SE; n=4).

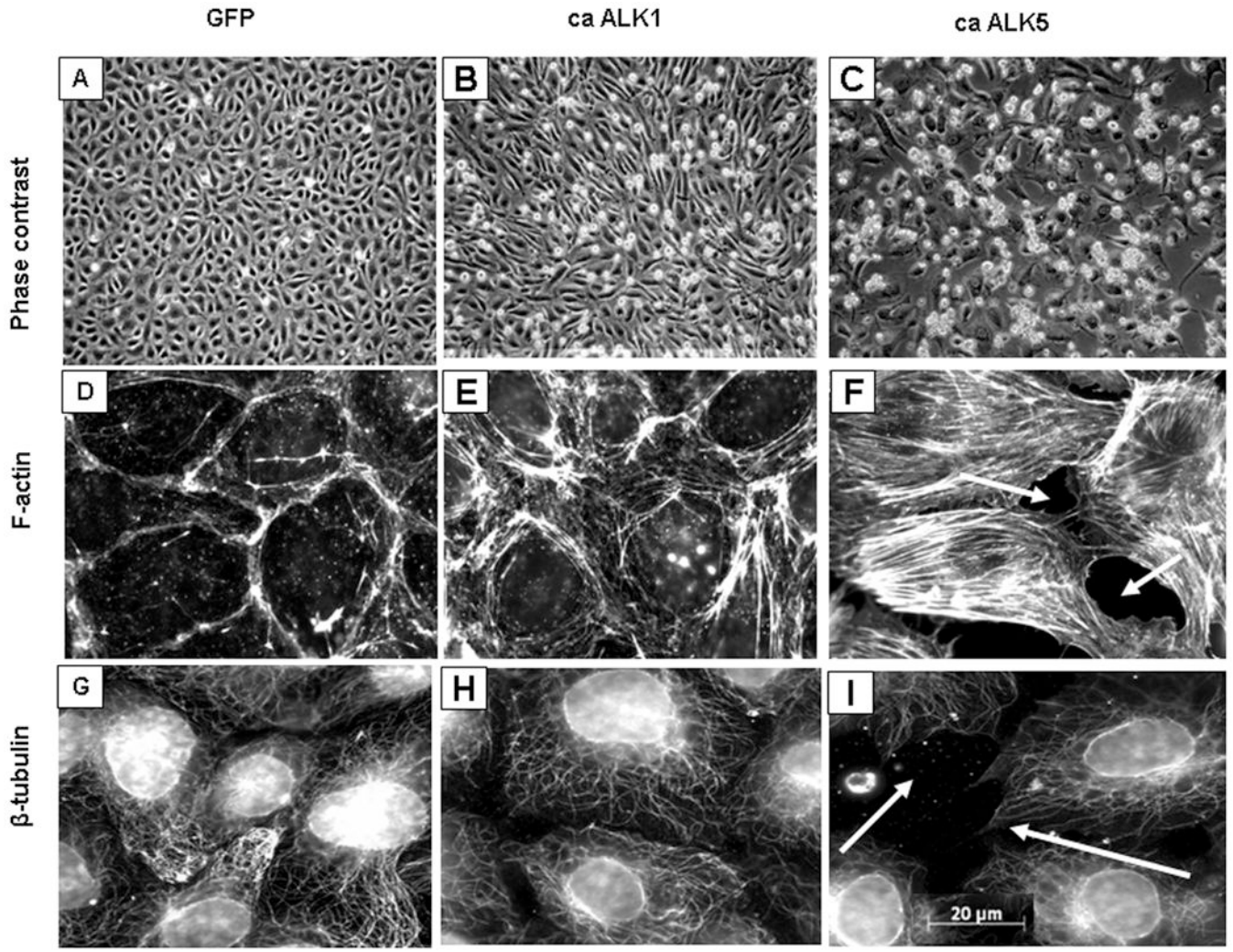

Figure 3. Infection with caALK1 and caALK5 has different effects on BPAEC monolayer integrity and cytoskeleton meshwork rearrangement

BPAEC grown on glass coverslips for 5 days were infected with GFP (A, D, G), caALK1 (B, E, H) or caALK5 (C, F, I); (all 50m.o.i.) for 18 hrs. The cells were formalin-fixed, permeabilized with 0.1% Triton X-100 and stained for F-actin (D, E, F) and β-tubulin (G, H, I) as described in Methods. Arrows indicate the loss of the contacts between EC (Bars=20μm; n=3) (F, I)). Phase contrast microphotographs illustrate morphological alterations in EC monolayer induced by adenoviral infection (A, B, C) (original magnification ×100).

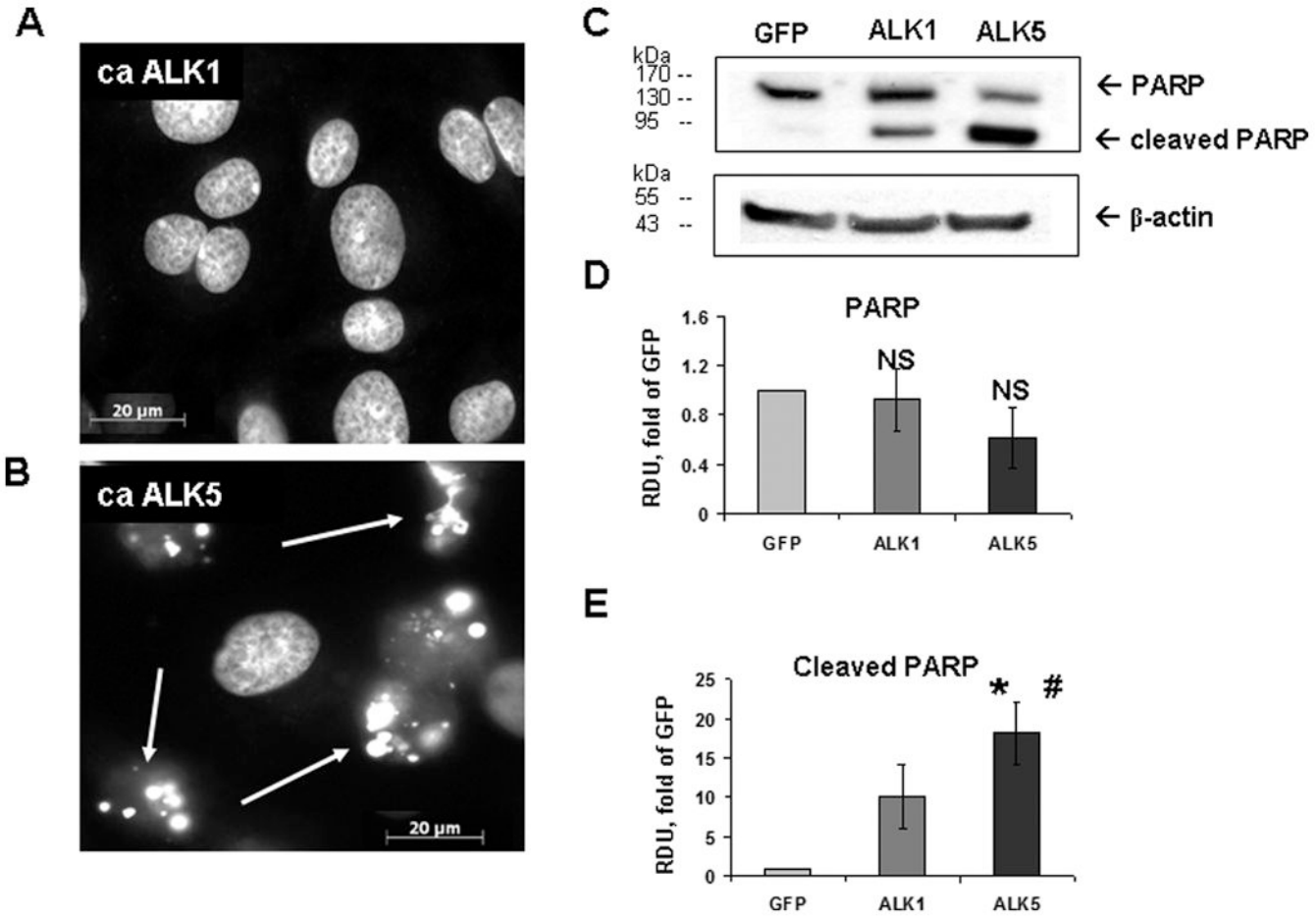

Figure 4. Adenoviral infection with caALK5 but not caALK1 induce BPAEC apoptosis

BPAEC were infected with 50 m.o.i. of caALK1 or caALK5 for 42 hrs. (A, B). Cells were fixed and stained with DAPI as described in Methods (bars=20μm; n=3). Arrows indicate nuclear fragmentation and chromatin condensation induced by caALK5 infection. (C) Cells were treated as described in (A, B) and cell lysates subjected to Western blot analysis for cleaved and uncleaved PARP levels. (D, E) PARP levels are presented as relative density units (RDU). Data were normalized to β-actin expression as control for equal protein loading and presented as fold increases in PARP levels compared to GFP treatment as control. (Data are mean±SE; n=4; *p<0.03, #p<0.02 compared with * - ALK1, or # - GFP; NS- not significant).

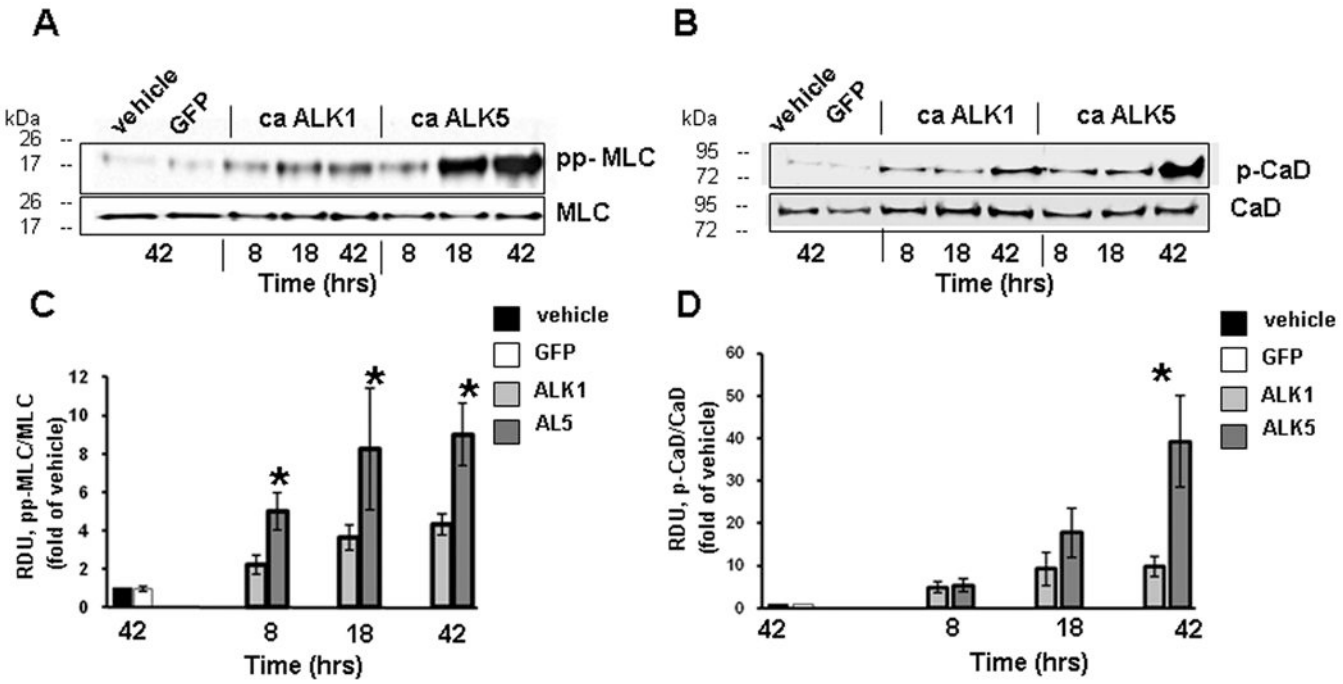

Figure 5. Adenoviral infection with caALK5 but not caALK1 induces MLC and caldesmon phosphorylation

BPAEC were infected with caALK1, caALK5, or GFP (50 m.o.i. for 42 hrs). Expression of diphospho-MLC and total MLC (A) and expression of phospho-caldesmon (p-CaD) and total caldesmon (CaD) were detected by Western blot with MLC, pp-MLC (Thr18/Ser19), CaD or p-CaD (Ser 789) Abs. (C, D). Effects of adenoviral infection on the activation of MLC and caldesmon phosphorylation were presented as relative density units (RDU). Data are the ratio of the levels of phosphorylated proteins to total proteins and a fold increase to vehicle treatment. (Data are mean±SE; **p*<0.05, compared with vehicle, n=4).

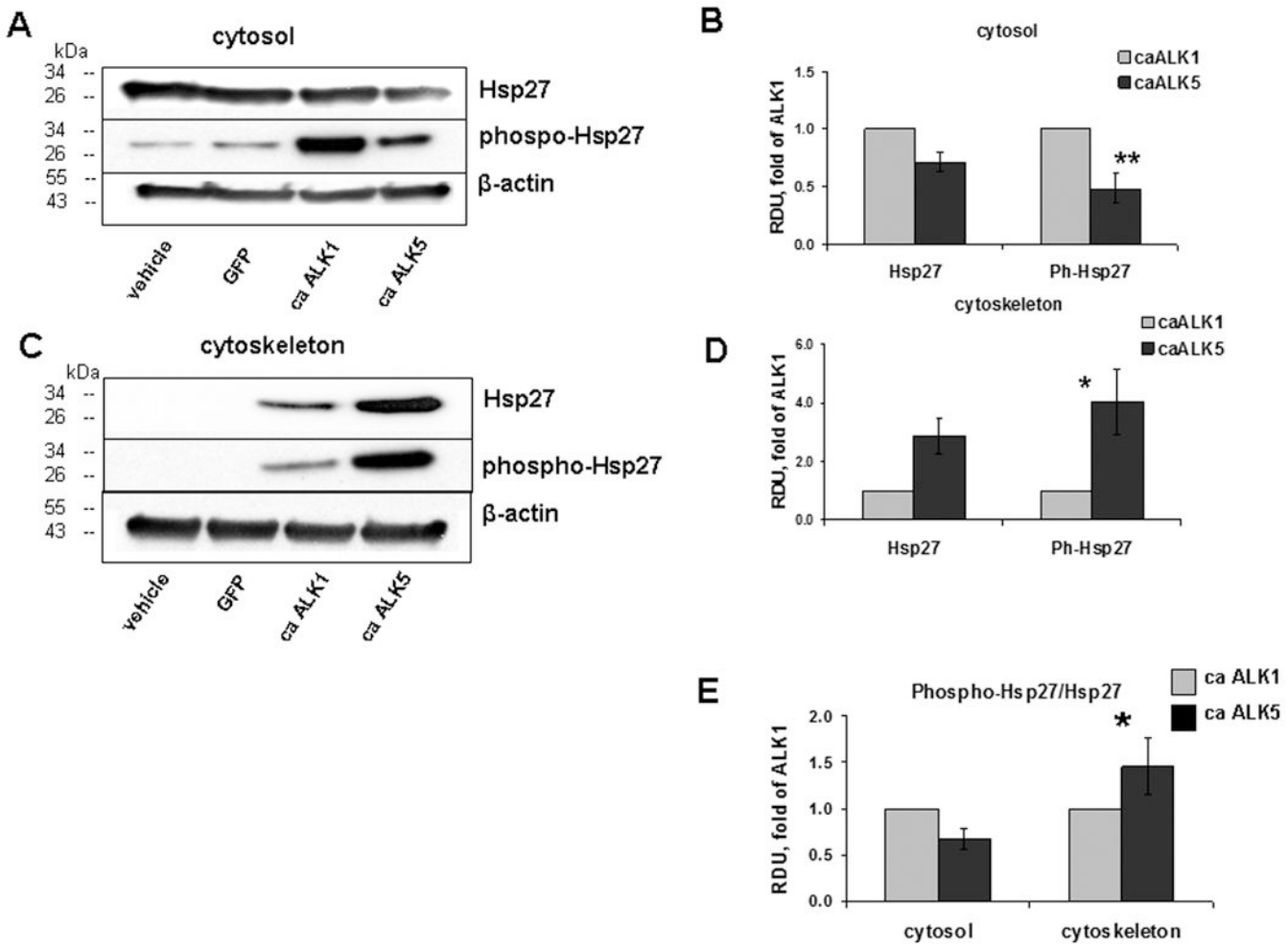

Figure 6. caALK5 infection, in contrast to caALK1 infection, targets Hsp27 accumulation and Hsp27 phosphorylation in the BPAEC cytoskeletal compartment

BPAEC were infected with ca ALK1, ca ALK5, or GFP (50 m.o.i.; 42 hrs). (A, B) Cells were lyzed and subcellular fractions prepared as described in Methods. Cytosolic and cytoskeletal fractions were analyzed for Hsp27 and phospho-Hsp27 levels by Western blot as described in Methods. Equal protein loading was confirmed by re-probing of membranes with β-actin Ab. (C, D,) Quantitative analysis of the level of Hsp27 and phospho-Hsp27 in cytosolic and cytoskeletal fractions presented as relative density units (RDU). Data presented as fold increases in Hsp27 or phospho-Hsp27 levels after caALK5 treatment as compared with caALK1 infection. (E) Ratio phospho-Hsp27/Hsp27 revealed level of phosphorylated Hsp27 in cytoskeleton comparing with cytosol after caALK1 and caALK5 infections. (Data are mean±SE; *p<0.05, effect of caALK5 treatment in cytoskeleton versus cytosol, n=4).

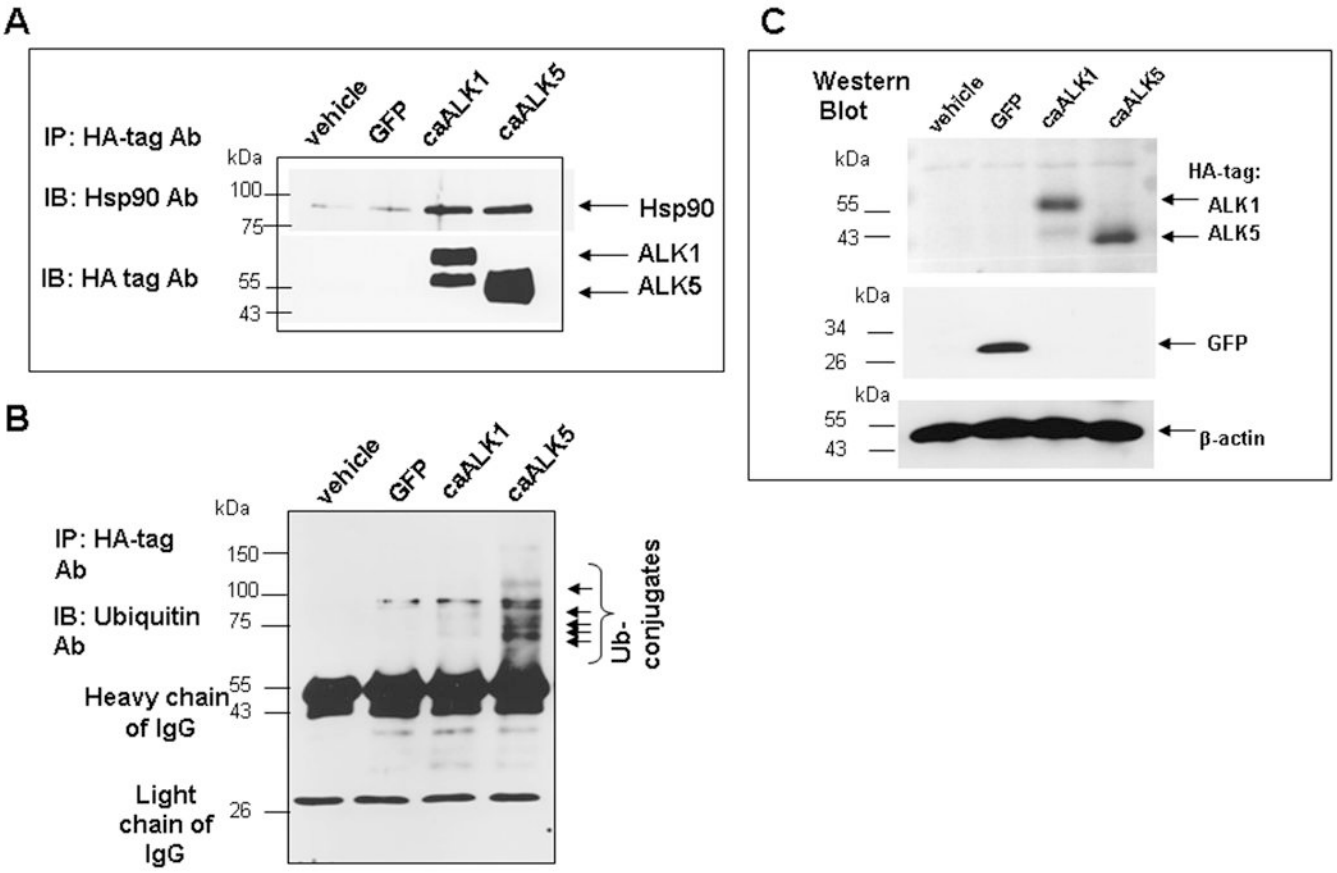

Figure 7. ALK1, ALK5 and ubiquitinated ALK5 interact with Hsp90

BPAEC cultured for 5 days were infected with caALK1, caALK5, or GFP (50 m.o.i. for 18 hrs). Whole cell lysates were prepared and immunoprecipitated with HA-tag-specific Ab as described in Methods. Precipitates were subjected to Western blot analysis with Hsp90-specific, HA-tag-specific (A) or ubiquitin-specific Ab (B). Isotype-matched IgG_1 was used as a control for specifity of immunoprecipitation. (C) Western blot analysis of whole cell lysates with HA-tag-specific, GFP-specific or b-actin specific Ab. (n=3).

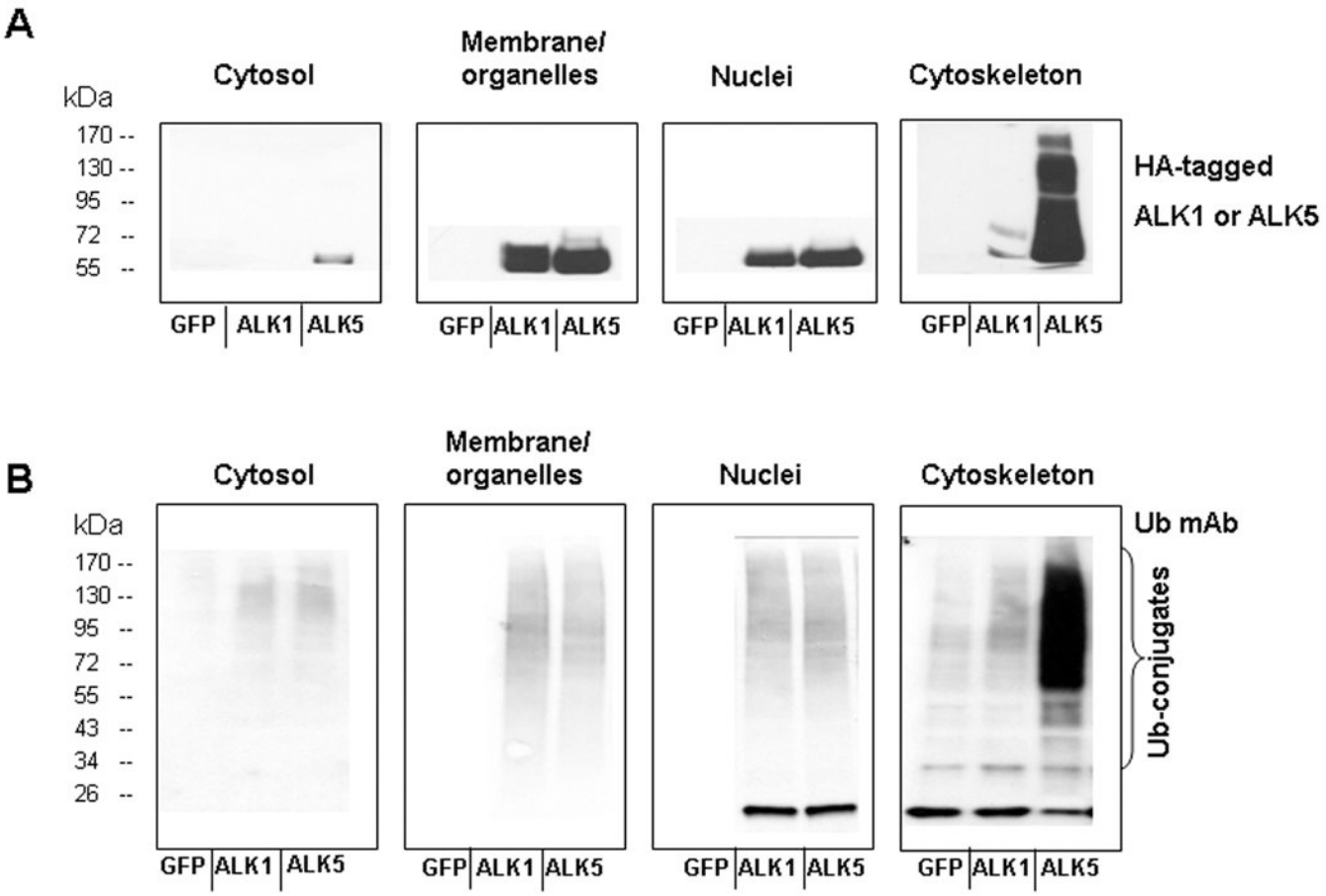

Figure 8. caALK5 infection, in contrast with caALK1 infection results in specific accumulation of ubiquitinated caALK5 in the cytoskeleton

BPAEC were infected with caALK1, caALK5, or GFP (50 m.o.i.; 42 hrs). Cells were harvested and subcellular fractions isolated as described in Methods. Equal amounts of protein were loaded and subjected to Western blot analysis with anti-HA-tag Ab (A) or anti-ubiquitin Ab (B). (n=4).

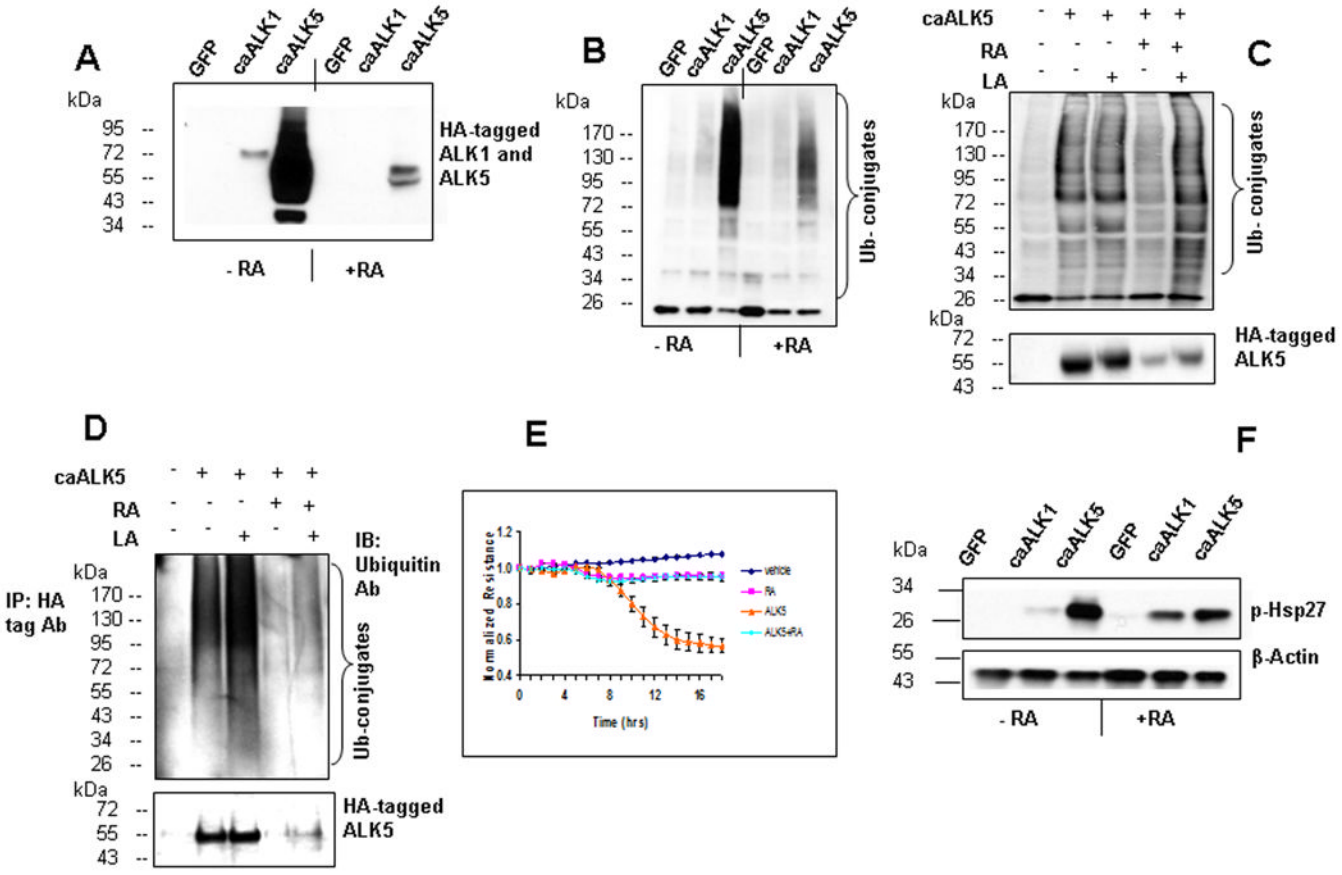

Figure 9. Hsp90 inhibitor RA prevents BPAEC functional alterations induced by caALK5 infection via mechanism requiring ubiquitinated caALK5 proteasome degradation

(A, B) Cytoskeleton fractions were isolated after caALK1 or caALK5 infection in the presence or absence RA (1 μg/ml) as described in Methods. caALK accumulation in the cytoskeleton fraction was examined by Western blot analysis with HA-tag specific Ab (A) or anti-ubiquitin Ab (B). (C) BPAEC were treated as in (A, B) in the presence of RA (1 μg/ml), LA (5 μM), or both as indicated. Cytoskeletal fractions were analyzed by Western blot with anti-ubiquitin Ab. (D) BPAEC were treated as in (A, B) in the presence of RA (1 μg/ml), LA (5 μM) or both as indicated, or with caALK5 alone. Cytoskeleton fractions were immunoprecipitated with HA-tag specific Ab. Expression of ubiquitinated caALK5 was examined with anti-ubiquitin Ab by Western blot. (E) BPAEC permeability was monitored by measuring TER after caALK5 infection in the presence or absence of RA (1 μg/ml). (F) BPAEC were infected with caALK1 and caALK5 as described in (A). Cytoskeleton fractions were prepared and examined by Western blot with anti-phospho-Hsp27 Ab. β-Actin was used as a control for equal protein loading. A-F; n=4.

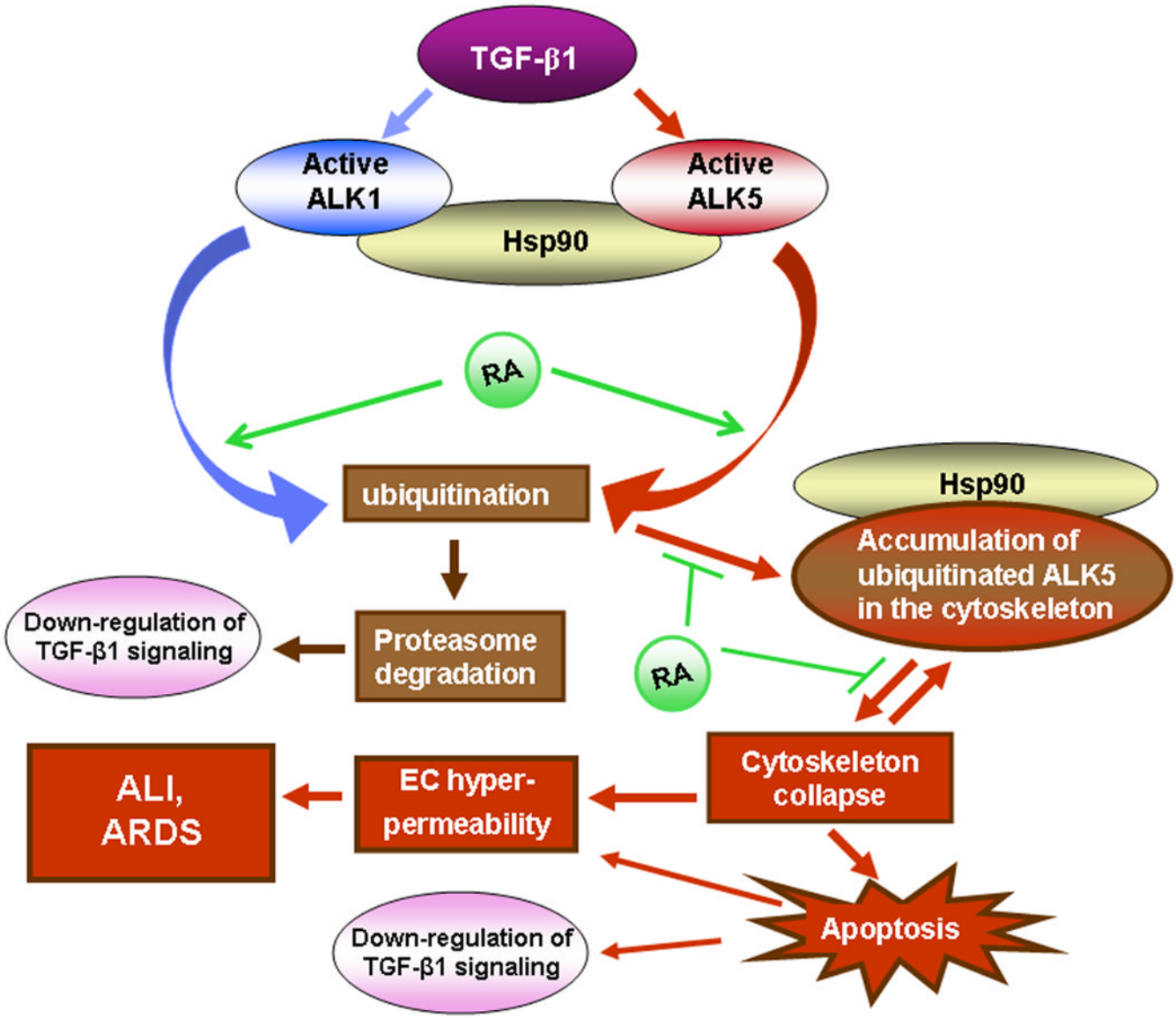

Figure 10. Hypothetical model of the regulation of endothelial barrier function by activated ALK1 and ALK5

ALK1 and ALK5 are proteins that interact with Hsp90. Subsequent to overexpression and persistent activation; they are subjected to ubiquitination and proteasomal degradation to maintain “normal” physiologically relevant responses to stressful stimuli. In contrast with caALK1, (pathway on the left) caALK5 is not subjected to proteasomal degradation (proteasomal insufficiency?), leading to accumulation of ubiquitinated AKL5 in cytoskeleton (pathway on the right). Ubiquitinated ALK5 aggregates can induce tubulin disruption, F-actin stabilization, and stress fiber formation, leading to the formation of a pathological loop that maintains compromised EC function. In contrast, activated ALK1 has no effect on cytoskeleton-dependent trafficking to the proteasome, and thus activated ALK1 is eliminated via degradation and does not induce EC barrier dysfunction. The mechanism of accumulation of ubiquitinated caALK5 is mediated by chaperone Hsp90. We hypothesize that persistent activation of overexpressed ALK5 is the molecular mechanism controlling TGF-β1-dependent EC permeability that plays a role in the pathogenesis of ALI and ARDS.

The Hsp90 inhibitor radicicol (RA) promotes proteasome degradation of AKL5 and prevents EC hyperpermeability.